SUPPLEMENTARY INFORMATION

From Melamine-Resorcinol-Formaldehyde to Nitrogen-Doped Carbon Xerogels with Micro- and Meso-pores for Lithium Batteries

Xichuan Liu,[a] Shaomin Li,[a] Jun Mei,[a] Woon-Ming Lau,[a] Rui Mi,[a] Yinchuan Li,[a] Hao Liu,*[a] and Limin Liu[b]

[a] Chengdu Green Energy and Green Manufacturing Technology R&D Center, Chengdu Development Center of Science and Technology, China Academy of Engineering Physics, Chengdu, Sichuan.

[b] Beijing Computational Science Research Center, Beijing 100084
E-mail: mliuhao@gmail.com

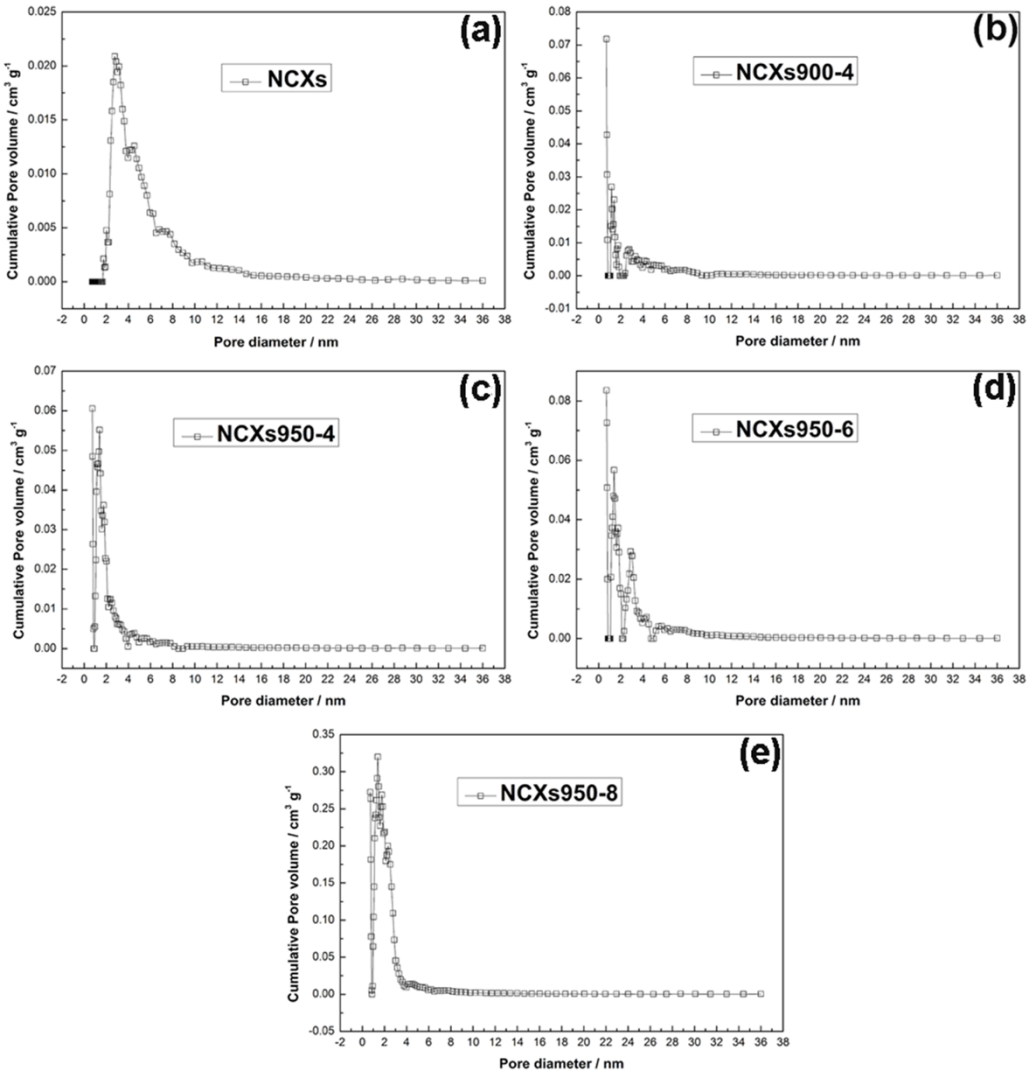

Fig. S1 The pore-size distribution cure of the multi-scaled porous NCXs.

The corresponding pore size distribution by nitrogen adsorption and desorption isotherms of the multi-scaled porous NCXs is shown in Fig. S1. After carbon dioxide activation, more micropores are created, designating the major presence of 2-nm pores.

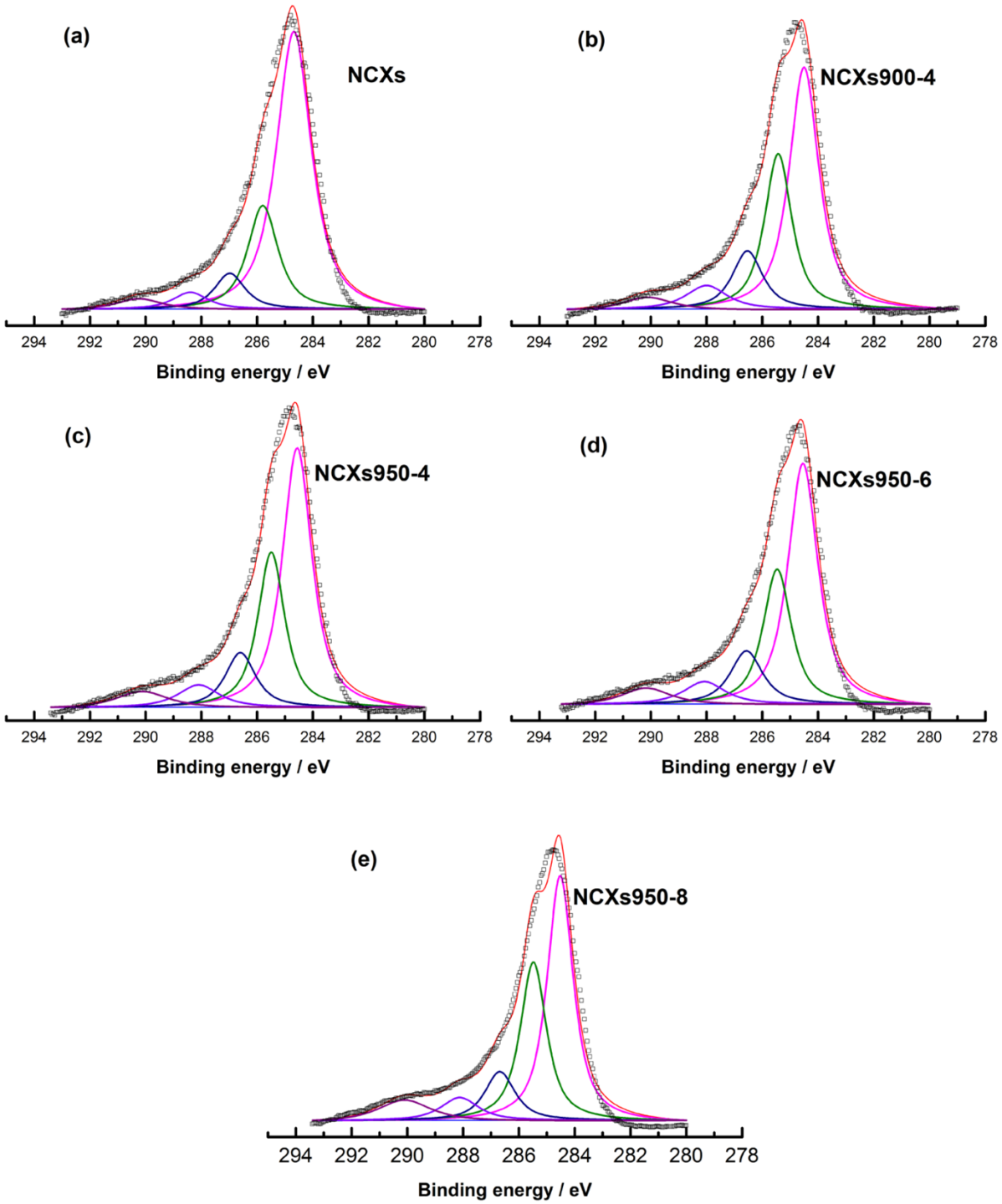

Fig. S2 XPS C1s spectra of the multi-scaled porous NCXs.

The chemical state analysis of carbon in NCXs is shown in the following figure. The C1s spectra for the multi-scaled porous NCXs are deconvoluted into five components as shown in Fig. S2. The contribution at around 284.5 eV can be ascribed to the presence of C-C bonds in graphitic carbon. A peak at around 285.3 eV is related to the presence of sp^3-like defects in the main graphitic structure of CXs and NCXs. The peak at around 286.6 can be related to C-O or C-N, and that at 288.1 eV to C=O. The weak and band at around 290 eV is likely due to the presence of carboxylic carbon.

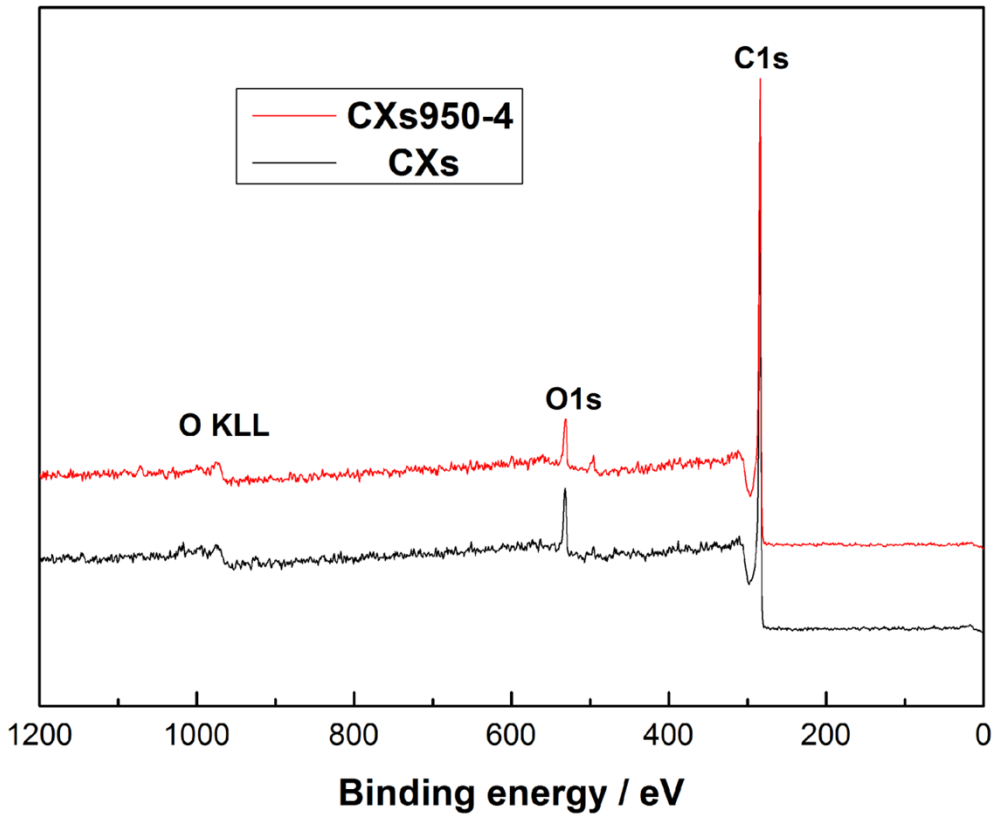

Fig. S3 XPS spectrum of the CXs (a) and CXs950-4 (b).

Table S1 Elements incorporation in NCXs and CXs in atomic percents.

	C (at. %)	**O** (at. %)	**N** (at. %)	**O/C (%)**
NCXs	89.0	6.2	4.8	6.97
NCXs900-4	90.0	6.4	3.6	7.11
NCXs950-4	92.2	5.5	2.3	5.97
NCXs950-6	93.3	4.6	2.1	4.93
NCXs950-8	94.2	4.1	1.7	4.35
CXs	92.7	7.3	--	7.87
NCXs950-4	94.1	5.9	--	6.27

The analysis shows the presence of some residual oxygen in the xerogels, which is indeed consistent with the detection of oxygen in the survey XPS scans shown in Fig. 4 and Fig. S3. The presence of residual oxygen is not surprising because oxygen is abundant in the precursor gels. During carbonization, most oxygen atoms are consumed by the oxidation reactions with carbon but some of them are expected to present in the resultant CXs or NCXs, for terminating and stabilizing carbon atoms at the surface and defect sites of the carbonaceous body. Some of the detected residual oxygen may also be oxygen-containing species chemisorbed on CXs or NCXs due to their good absorbent nature. Although residual oxygen is always present in NCXs, by comparing CXs with residual oxygen and NCXs with residual oxygen, we have found no correlation between the presence of residual oxygen to the observed improvement of electrochemical performance of NCXs.

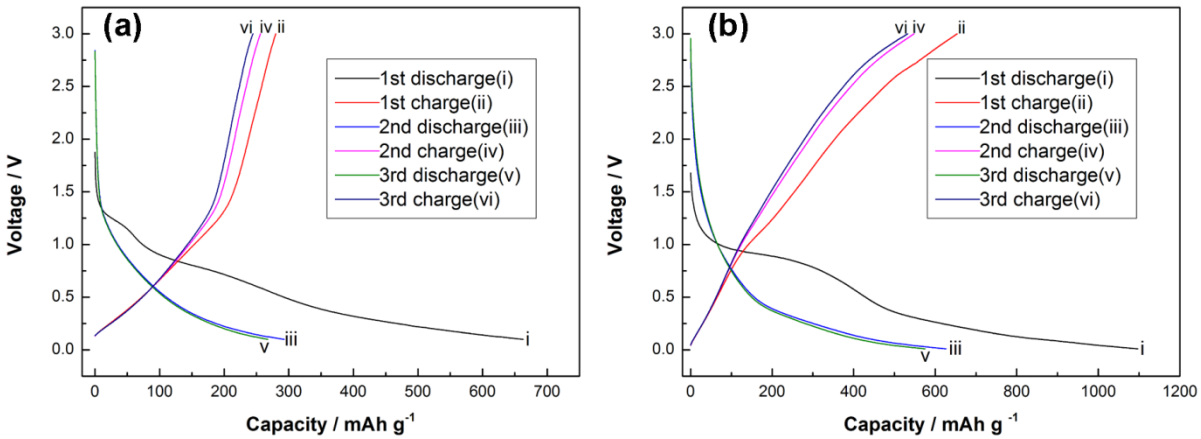

Fig. S4 Discharge/charge profiles of the CXs (a) and CXs950-4 (b).

The discharge/charge profiles of the CXs and CXs950-4 are presented in Fig. S4. During the first discharge process, the voltage drops rapidly and forms a plateau at about 0.75 V, which is observed in the first cycle, indicating the formation of a solid electrolyte interface (SEI) layer on the relatively large specific surface area of the sample. The other plateau around 0.1 V should be attributed to the intercalation of lithium ions in carbon xerogels materials. In the following cycles, all samples exhibit stable reversible capacities.

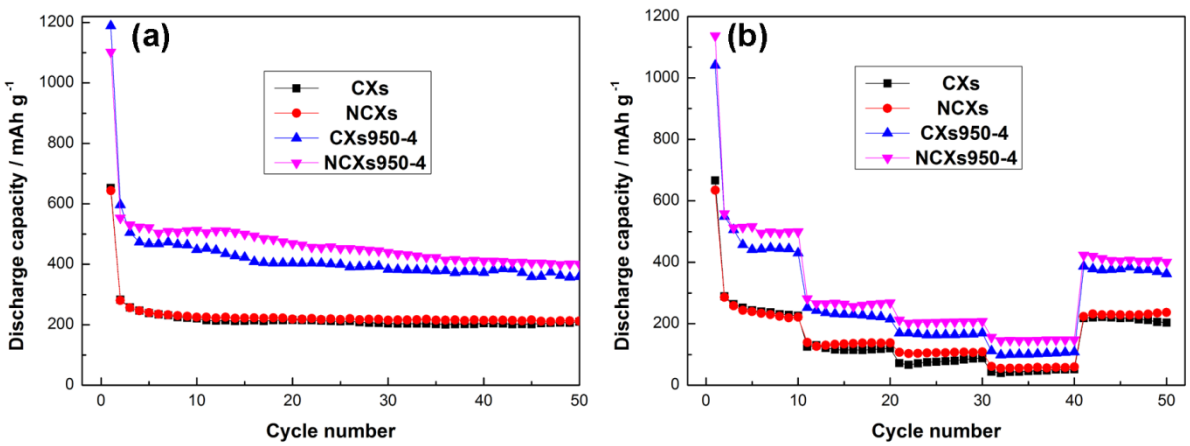

Fig. S5 Cycling performance and rate capability of the CXs and NCXs.

The cycle performance and rate capability of the CXs and activated products (CXs950-4) without nitrogen-doping are presented in Fig. S5. These results indicate that at the same activation condition, nitrogen-doped NCXs consistently exhibit better electrochemical properties i. e. specific capacity and rate capacity, than their CXs counterparts. Hence, nitrogen-doping is important.

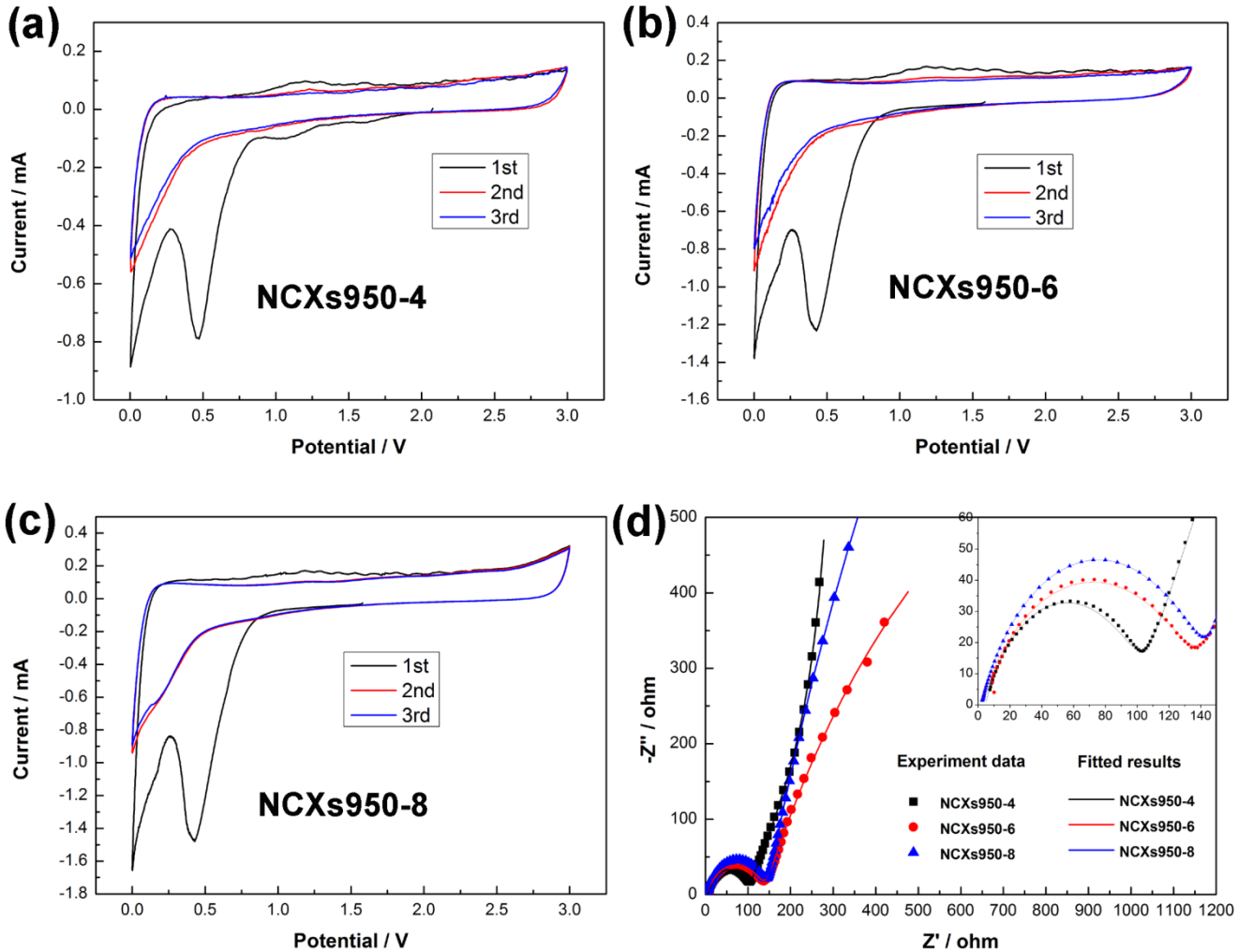

Fig. S6 Cycling performance (a, b, c) and Nyquist plots (d) of the multi-scaled porous NCXs.

Table S2 Kinetic parameters of the activated NCXs .

Sample	R_e (ohm)	R_f (ohm)	R_{ct} (ohm)
NCXs950-4	2.6	79.9	113.8
NCXs950-6	1.3	97.7	215.4
NCXs950-8	2.1	123.9	260.0

The fitting values are derived from equivalent circuit.

These electrochemical processes of NCXs950-4 are consistent with those of the NCXs950-6 and NCXs950-8 samples shown in Fig. S6. Compared with the second and third cycles of the CV curves, no significant curve shift is observed for both the NCXs and the activated samples, which implies good cycling performance. In addition, the composite resistance values of R_{ct}+R_f are increase with activation duration which is attributed the loss of the perfect sp^2 structure of graphite and a yield of defective graphite and other sp^3-like carbon strctures.